

# Spectroscopic Properties of Odd-Mass Rare-Earth Nuclei in the HF+BCS Approach Using the Density-Dependent Delta Interaction

Nor Anita Rezle, Nurhafiza Mohamad Nor, Meng-Hock Koh

*Department of Physics, Faculty of Science,  
Universiti Teknologi Malaysia, 81310 Johor Bahru, Johor, Malaysia*

(Received: 9.2.2018 ; Published: 25.9.2018)

**Abstract.** Pairing correlations play an important role in the description of nuclear properties such as binding energy, odd-even mass staggering (OES) and it has continued to be important when going towards extremely deformed nuclear shapes. It is therefore important that pairing is treated in the best way possible within any theoretical framework. In this work, we present an exploratory study investigating the effect of using a pairing interaction called the density dependent delta interaction (DDDI) in the calculation of band-head energies of odd-mass nuclei. In this preliminary work, the pairing strengths were fitted to the OES of  $^{162,163,164}\text{Gd}$  isotopes assuming that the proton and neutron pairing strengths to be similar. Calculations of the odd-mass nuclei were performed by blocking one single-particle state in which its third-component of the single-particle total angular momentum and parity matches the intended experimental nuclear spin and parity. The optimal pairing strength was found to be  $1216 \text{ MeV fm}^3$ . Theoretical data of intrinsic and spectroscopic quadrupole moment, magnetic moment and band-head for odd-mass nuclei are presented. Disagreement between theoretical band-head of  $^{161}\text{Gd}$  with that of experimental data is probably due to its intrinsic nature and to be fixed with rotational correction.

**Keywords:** Pairing correlation, HF+BCS, Density dependent delta interaction

## I. INTRODUCTION

In the mean-field approach, pairing correlations are often treated within the Hartree-Fock Bardeen-Cooper Schrieffer (HF+BCS) or the Hartree-Fock-Bogoliubov (HFB) framework. While HFB is a more comprehensive framework treating both the nucleon-nucleon and pairing interactions on the same footing, it was found that the HF+BCS performs just as well in many cases. The most common pairing interaction used in the HF+BCS approach is the seniority force [1, 2]. Recently, Ref. [1] adopted seniority force in HF+BCS calculations for odd-mass actinide nuclei and presented a set of pairing strengths for each SIII and SkM\* interactions and produced rotational band heads of deformed odd-neutron nuclei with good agreement to that experimental ones. A study of inner fission barrier with seniority force within HF+BCS in Ref. [3] stated an agreement of low energy spectra of actinide nuclei. Despite that, the experimental data for actinide region is quite lacking hence it is better to move to other region with more experimental data, for example the rare-earth region.

It is generally agreed that the seniority force is too simple and a better pairing interaction should be used. Ref. [4] stated that seniority force having to extrapolate the pairing strengths away from nuclear stability line may not be a good idea since it is obtained near the stability line. Author of Ref. [4] proposed another choice of pairing treatment called density-dependent delta interaction (DDDI) that has now been adopted in mean field study to treat pairing in HF+BCS, HFB and for excited state, the quasiparticle random phase approximation (QRPA). Ref. [4] stated that DDDI offer better extrapolation compared to that of seniority force especially when approaching the drip lines. Recent work from Ref. [5] adopted DDDI in surface and volume pairing to study pairing and deformation effects on excited state of deformed rare-earth even-even <sup>152,154,156</sup>Sm isotopes in which mean field and pairing are treated within HF+BCS approach. Adopting SLy6 Skyrme parameter, the authors of Ref. [5] fitted different pairing strengths for volume ( $V_n = -288.5 \text{ MeV fm}^3$  and  $V_p = -298.8 \text{ MeV fm}^3$ ) and surface pairing with the latter having higher pairing strengths of  $V_n = -864.2 \text{ MeV fm}^3$  and  $V_p = -1053.12 \text{ MeV fm}^3$  than the former. Comparing surface with volume pairing, the authors noticed only small difference QRPA results. Meanwhile, in shape transition studies of Yb isotopes by Ref. [6], the authors performed HF+BCS with SLy4 Skyrme parameter and DDDI, comparing it with density independent delta interaction shows that DDDI predicts the most rapid spherical to prolate shape. Both studies show that DDDI is deemed compatible in treating pairing force in deformed nuclei. In this work, we are interested to investigate the effect of using a more realistic pairing interaction called DDDI in describing nuclear properties of some odd-mass rare-earth nuclei. We will discuss the HF+BCS theoretical framework of our calculation in the next section and pairing strengths fit will be discussed in the third section of this paper. The fitted pairing strengths are then used to perform single-particle state blocking which will be presented in the Discussion section.

## II. THEORETICAL FRAMEWORK

The effective nucleon-nucleon interaction entering the HF part is approximated here to a phenomenological Skyrme interaction. When using the Skyrme interaction, the total energy of the nucleus,  $E$  can be written as the integral of the Hamiltonian density  $H(r)$  such that

$$\begin{aligned} E &= \int H(r) dr \\ &= \int H_{kin}(r) + H_c(r) + H_{DD}(r) + H_{s.o}(r) + H_{Coul}(r) \end{aligned} \quad (1)$$

The Hamiltonian density on the other hand is written in terms of some local densities which are either time-odd or time-even depending on the action of the time reversal operator. The local densities on the other hand depend on the single-particle wave functions. In the case of ground state of an even-even nucleus, the time-odd local densities namely the current density  $j(r)$ , the spin kinetic density  $T_\mu(r)$  and the spin density  $s(r)$  vanish identically. Only the time-even densities contribute to the Hamiltonian density in such situation. The contribution from the Coulomb interaction is taken into account through the Coulomb term given as:

$$H_{Coul}(r) \approx \frac{1}{2} \rho_P(r) V_{CD}(r) - \frac{3}{4} e^2 \left(\frac{3}{\pi}\right)^{1/3} \rho^{4/3}(r) \quad (2)$$

The first term on the right is the direct Coulomb term and the potential is given as

$$V_{CD} = e^2 \int dr' \frac{\rho_p(r')}{\|r-r'\|} \quad (3)$$

The second term arises due to the exchange term treated within a local density approximation.

However, the unpaired nucleon in the ground state of an odd-mass nucleus causes the time – reversal symmetry to be broken. The time-odd local densities do not vanish in this case and contribute to the lifting of the Kramer’s degeneracy inherent to the even-even nucleus mentioned above.

Varying the Hamiltonian density with respect to the single-particle wave function, one then obtains the HF equation to be solved.

$$\begin{aligned} \left\langle r \left| \hat{h}_{HF}^{(q)} \right| \phi_k \right\rangle = & -\nabla \cdot \left( \frac{\hbar^2}{2m_q^*} \nabla(\phi_k)(r) + \left( U_q(r) + \delta_{qp} U_{COU}(r) \right) \right) (\phi_k)(r) \\ & + iW_q(r) \cdot (\sigma \times \nabla(\phi_k)(r)) - i \sum_{\mu,\nu} \left[ W_{q,\mu\nu}^{(j)}(r) \sigma_\nu \nabla_\nu(\phi_k)(r) \right. \\ & \left. + \nabla_\mu \left( W_{q,\mu\nu}^{(j)}(r) \sigma_\nu(\phi_k)(r) \right) \right] - \frac{i}{2} \left[ A_q(r) \cdot \nabla(\phi_k)(r) + \nabla \cdot \left( A_q(\phi_k)(r) \right) \right] \\ & + S_q(r) \cdot \sigma(\phi_k)(r) - \nabla \cdot \left[ \left( C_q(r) \cdot \sigma \right) \nabla(\phi_k)(r) \right] \end{aligned} \quad (4)$$

where  $m^*$  is effective mass,  $U_q$  is central-density-dependent field,  $U_{cou}$  is the Coulomb field,  $W_q$  is the spin-orbit field and  $W_{q,\mu\nu}^{(j)}$  is the spin-orbit field with  $q$  as the nuclear charge state with  $q = p$  for proton and  $q = n$  for neutron. The time-odd fields which vanish are spin field  $S_q$ , current field  $A_q$ , and spin-gradient,  $C_q$  [7, 8].

In addition to the HF contribution, the contribution of the pairing correlations is accounted using the BCS method. In the BCS framework, the pairing interaction is approximated to the DDDI given as:

$$V^{(q)}(r_1, r_2) = V_0^{(q)} \left[ 1 - \eta \left( \frac{\rho}{\rho_0} \right)^\gamma \right] \delta(r_1 - r_2) \quad (5)$$

whereby  $\rho_0 = 0.16 \text{ fm}^{-3}$  is the saturation density,  $\rho$  is the total density and  $V_0^{(q)}$  is the pairing strength parameter to be determined. We consider here mixed pairing and thus the value of  $\gamma$  is fixed to 0.5 for all calculations with parameter  $\eta$  being fixed to 1.

At the end of BCS calculations the local densities are now written and multiplied by the  $v_k^2$ . Taking only the single-particle density as example, the density operator is now written as

$$\rho(r) = \phi_k^*(r') \phi_k(r) + \sum_{\substack{m>0 \\ m \neq 0}} v_k^2 \phi_k^*(r') \phi_k(r) \quad (6)$$

The occupation probability is obtained by constraining the BCS equation to reproduce the right particle number.

$$N_q = \sum_{\Omega_k > 0} v_k^2 \quad (7)$$

with

$$v_k^2 = \frac{1}{2} \left[ 1 - \frac{e'_k - \lambda}{[(e'_k - \lambda)^2 + \Delta^2]^{1/2}} \right] \quad (8)$$

The new values local densities are the feed into the HF equation. At each HF iteration, the BCS calculation is performed. The solution is repeated until convergence is reached.

For an odd-mass nucleus, the HF+BCS calculation is performed by blocking one single-particle state i.e. setting the occupation probability of this state to 1. The blocked state is chosen in such a way that the projection of the total angular momentum and parity correspond to the experimental nuclear spin.

### III. TECHNICAL ASPECTS

In the first stage of our HF+BCS calculations, parameter for Skyrme interaction SIII is selected with axial symmetry. This is due to the reliability of SIII in describing deformed rare-earth nuclei [9] and Ref. [8] showed that band head spectra agreed qualitatively with experimental data. We opted for isoscalar density-dependent delta interaction (DDDI) given by Equation (5) for the BCS pairing strength.

For this preliminary study, we have made a fit by adjusting the pairing strength  $V_0^{(q)}$  to reproduce the experimental odd-even mass staggering (OES) of  $^{162,163,164}\text{Gd}$  isotopes with formula shown in Equation (9). To simplify the calculation process, the neutron and proton pairing strengths are assumed to be the same.

$$\Delta^{(3)} = \frac{(-)^N}{2} [E(N - 1, Z) - 2E(N, Z) + E(N + 1, Z)] \quad (9)$$

$N$  is the number of odd neutron and  $Z$  is the number of proton.

Since single-particle states are expanded on harmonic oscillator basis with axial symmetry, a truncation is deemed necessary according to Ref. [10]. The basis size,  $N_0$  used throughout our work is 14 representing 15 shells for solution with spherical symmetry. The spherical harmonic oscillator constant,  $b$  and deformation parameter,  $q$  are optimized for ground state solution for two even-even nuclei and its average value is optimized for its odd neighbouring nuclei. The basis parameters ( $N_0$ ,  $b$  and  $q$ ) obtained from the seniority force calculation [11].

Table 1 shows  $^{163}\text{Gd}$  OES results of SIII parameter and mixed pairing of DDDI for different pairing strengths. The optimal pairing strength fitted to reproduce experimental OES is  $V_n = V_p = 1216 \text{ MeV fm}^3$ . Least amount of deviation of 0.01 MeV was found when compared to the experimental OES of which -0.67 MeV [12].

**TABLE 1.** Odd-even mass difference  $\Delta^{(3)}$  for  $^{163}\text{Gd}$  at different pairing strengths. Both theoretical and experimental results are presented.

Vn	Vp	Binding Energy (MeV)			$\Delta^{(3)}$ OES (MeV)	
		Gd-162	Gd-163	Gd-164	THEO	EXP
1215	1215	1316.73	1322.70	1330.67	-1.00	
1216	1216	1316.84	1323.11	1330.69	-0.66	-0.67
1217	1217	1316.96	1323.52	1330.70	-0.31	

The fitted pairing strengths are then used for blocked calculations for odd-mass nuclei around  $^{162}\text{Gd}$ .

#### IV. RESULTS AND DISCUSSIONS

Table 2 shows the intrinsic charge quadrupole moment  $Q_0$  of even-even nuclei  $^{162,164}\text{Gd}$ . We are unable to compare our data due to the absence of experimental data for both nuclei [13].

**TABLE 2.** Intrinsic charge quadrupole moment,  $Q_0$  of even-even nuclei,  $^{162,164}\text{Gd}$ .

Nucleus	$Q_0$ (barn)
Gd-162	7.19
Gd-164	7.47

Table 3 shows the intrinsic charge quadrupole moment,  $Q_0$  and spectroscopic charge quadrupole moment  $Q^{(s)}$  of even-proton nuclei and odd-proton nuclei calculated with Equation (10) with blocked single-particle state,  $K^\pi$  given by experiment values obtained from Ref. [14]. A constrained calculation was performed for  $^{161}\text{Eu}$  with  $Q_{20} = 1853.933 \text{ fm}^2$  and  $Q_{40} = 0.2318 \text{ b}^2$ . There is no experimental data for quadrupole moment available for these nuclei hence we are unable to compare our data with previous works [13].

$$Q^{(s)} = \frac{3K^2 - I(I+1)}{(K+1)(2I+3)} Q_0 \quad (10)$$

where the quantum number of the nuclei,  $K = I$ .

**TABLE 3.** Intrinsic charge quadrupole moment,  $Q_0$  and spectroscopic charge quadrupole moment,  $Q^{(s)}$  of odd-neutron nuclei  $^{161,163}\text{Gd}$  and odd-proton nuclei  $^{161}\text{Eu}$  and  $^{163}\text{Tb}$ .

Nucleus	$K^\pi$	$Q_0$ (barn)
Gd-161	$5/2^-$	7.19
Gd-163	$7/2^+$	7.27
Eu-161	$5/2^+$	7.29
Tb-163	$3/2^+$	7.62
Nucleus	$K^\pi$	$Q^{(s)}$ (barn)
Gd-161	$5/2^-$	2.57
Gd-163	$7/2^+$	3.39
Eu-161	$5/2^+$	2.60
Tb-163	$3/2^+$	1.52

Experimental values for intrinsic and total magnetic moment are also unavailable, so we could only present the theoretical values in Table 3 for odd-neutron and odd-proton nuclei [13]. Equation (11) and (12) show the total magnetic moment,  $\mu$  and collective magnetic moment,  $\mu_{coll}$  respectively

$$\mu = \mu_{intr} + \mu_{coll} \quad (11)$$

$$\mu_{coll} = \frac{K}{K+1} g_r \quad (12)$$

where intrinsic magnetic moment,  $\mu_{intr}$  is given in Equation (13)

$$\mu_{intr} = \frac{K}{K+1} \langle \Psi | \hat{\mu}_z | \Psi \rangle \tag{13}$$

where  $\langle \hat{\mu}_z \rangle$  is the expectation value of magnetic dipole moment operator on the axis of symmetry, z while  $\Psi$  is the normalized nuclear state with good quantum numbers. Meanwhile, the  $g_r$  in Equation (12) refers to the gyromagnetic ratio, calculated microscopically within the Inglis-Belyaev approximation in the underlying even-even nucleus [15].

**TABLE 4.** Intrinsic magnetic moment,  $\mu_{intr}$  gyromagnetic ratio,  $g_r$ , collective magnetic moment,  $\mu_{coll}$  and total magnetic moment,  $\mu$  of odd neutron nuclei  $^{161,163}\text{Gd}$  and odd-proton nuclei  $^{161}\text{Eu}$  and  $^{163}\text{Tb}$ .

Nucleus	$K^\pi$	$\mu_{intr} (\mu_N)$	$g_r$	$\mu_{coll}$	$\mu (\mu_N)$
Gd-161	$5/2^-$	0.64	0.08	0.25	0.89
Gd-163	$7/2^+$	-0.85	0.43	-0.44	-1.09
Nucleus	$K^\pi$	$\mu_{intr} (\mu_N)$	$g_r$	$\mu_{coll}$	$\mu (\mu_N)$
Eu-161	$5/2^+$	0.72	0.28	0.28	1.00
Tb-163	$3/2^+$	1.90	0.24	1.26	3.16

However, using Equation (14) we calculated the excitation energy  $E_{K\pi\alpha}^*$  of  $^{161}\text{Gd}$  and the values tabulated Table 5. The experimental ground-state  $E_{K\pi\alpha}^{(gs)}$  here is at  $K^\pi = 5/2^-$ . The experimental values of  $K^\pi$  and  $E_{K\pi\alpha}$  are obtained from Ref. [12].

$$E_{K\pi\alpha}^* = E_{K\pi\alpha}^{(gs)} - E_{K\pi\alpha} \tag{14}$$

**TABLE (1).** Excitation energies of Gd-161.

Nucleus	$E_{K\pi\alpha}^* (\text{MeV})$		
	$K^\pi$	THEO	EXP
Gd-161	$5/2^-$	0	0
	$1/2^-$	2.24	0.355
	$7/2^+$	2.02	0.51

Based on Table 5, there is a big difference between our value and the experimental one at  $K^\pi = 1/2^-$  state by 1.885 MeV. At  $K^\pi = 7/2^+$  state, our value differ by 1.51 MeV. Nevertheless, both  $5/2^-$  values agree with each other. Figure 1 shows a band head spectra based on our data in Table 5. It can be observed that  $K^\pi = 7/2^+$  and  $K^\pi = 1/2^-$  states are at higher energy than that of experimental  $K^\pi = 7/2^+$  and  $K^\pi = 1/2^-$  states.

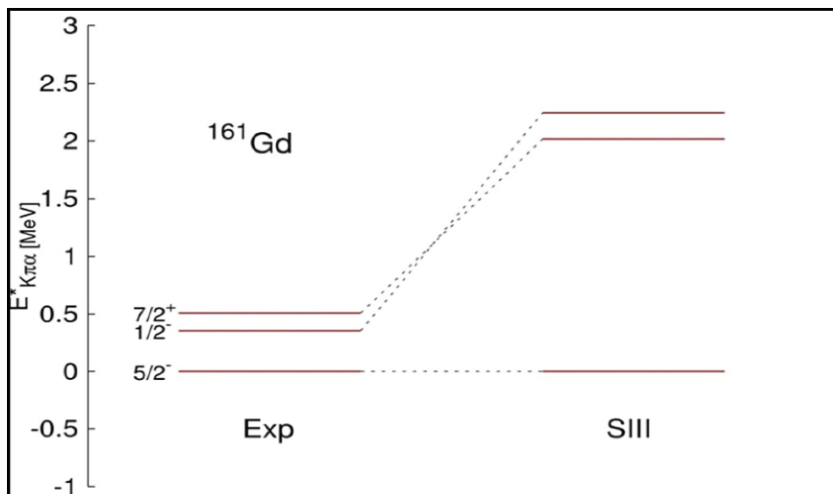


FIGURE 1. Comparison of band head spectra of  $^{161}\text{Gd}$  with SIII parameter and experimental data.

## V. CONCLUSIONS

We have presented neutron OES on  $^{163}\text{Gd}$  nuclei using self-consistent HF+BCS calculation with SIII Skyrme parameter and mixed pairing of DDDI. Optimal pairing strengths to reproduce the experimental OES are fitted. Single particle state blocking has been conducted for 4 neighbouring nuclei of  $^{162}\text{Gd}$ . We are unable to compare some of our findings i.e. quadrupole moment, intrinsic and total magnetic moment due to lack of experimental data. The band head energies appear to disagree with experimental data with slight difference at  $K^\pi = 7/2^+$  and  $K^\pi = 1/2^-$ . This could be because of the intrinsic nature of our calculation. Future recommendation is to include rotational correction to produce result with better agreement with experimental data.

This work could be extended by exploring more odd nuclei in the rare-earth region. Also, a better pairing treatment such as the highly truncation diagonalization approach (HTDA) could be used to study pairing correlation in the isomeric and high spin states.

## ACKNOWLEDGMENTS

Nor Anita would like to thank the Universiti Teknologi Malaysia for providing financial support to present this work through the Potential Academic Staff (PAS) grant (grant number Q.J130000.2726.02K70). Nurhafiza would also like to acknowledge the same research grant for partial financial support for her postgraduate study. The authors appreciation also goes to the Ministry of Higher Education (MOHE) Malaysia for the financial support for this publication under the STEM Grant (vote no. A.J091002.5600.07397).

## REFERENCES

1. M. H. Koh, D. D. Duc, T. N. Hao, H. T. Long, P. Quentin, and L. Bonneau, *The European Physical Journal A*, **52**(1), 3 (2016).
2. Ebata, Shuichiro, and Takashi Nakatsukasa. *Physica Scripta* **92**(6), 064005 (2017).
3. Benrhabia, D. E. Medjadi, M. Imadalou, P. Quentin. *Physical Review C*. **96**(3), 034320 (2017).
4. F. Tondeur. *Nuclear Physics A*, **315**(3), 353-369 (1979).

5. A. Repko, J. Kvasil, V. O. Nesterenko, and P-G. Reinhard. *The European Physical Journal A* **53(11)**, 221 (2017).
6. Y. Fu, H. Tong, X. F. Wang, H. Wang, D. Q. Wang, X. Y. Wang, and J. M. Yao. *Physical Review C* **97(1)**, 014311 (2018).
7. P. Bonche, H. Flocard, and P. H. Heenen. *Nuclear Physics A*, **467(1)**, 115-135 (1987).
8. M. H. Koh, L. Bonneau, P. Quentin, T. N. Hao, and H. Wagiran. *Physical Review C*, **95(1)**, 014315 (2017).
9. J. Libert, and P. Quentin. *Physical Review C*, **25(1)**, 571 (1982).
10. H. Flocard, P. Quentin, A. K. Kerman, and D. Vautherin. *Nuclear Physics A*, **203(3)**, 433-472 (1973).
11. M. N. Nurhafiza, M. H. Koh, N. A. Rezle, P. Quentin, and L. Bonneau. *Jurnal Fizik Malaysia* **39(2)**, 30033-30037 (2018).
12. M. Wang, G. Audi, A. H. Wapstra, F. G. Kondev, M. MacCormick, X. Xu. and B. Pfeiffer. *Chinese Physics C*, **36(12)**, 1603 (2012).
13. N. J. Stone. *Atomic Data and Nuclear Data Tables* **111**, 1-28 (2016).
14. A. K. Jain, R. K. Sheline, P. C. Sood, and K. Jain. *Reviews of Modern Physics*, **62(2)**, 393 (1990).
15. L. Bonneau, N. Minkov, Dao Duy Duc, P. Quentin, and J. Bartel. *Physical Review C* **91(5)**, 054307 (2015).